IEEE Access
Multidisciplinary | Rapid Review | Open Access Journal

Received January 7, 2019, accepted January 14, 2019, date of publication January 25, 2019, date of current version February 20, 2019.

Digital Object Identifier 10.1109/ACCESS.2019.2895204

Subarray-Cooperation-Based Multi-Resolution Codebook and Beam Alignment Design for mmWave Backhaul Links

RENMIN ZHANG[1,2], (Student Member, IEEE), HUA ZHANG[1], (Member, IEEE), WEI XU[1], (Senior Member, IEEE), AND XIAOHU YOU[1], (Fellow, IEEE)

[1]National Mobile Communications Research Laboratory, Southeast University, Nanjing 210096, China
[2]Hunan Provincial Key Laboratory of Ecological Agriculture Intelligent Control Technology, Huaihua University, Huaihua 418008, China

Corresponding authors: Hua Zhang (huazhang@seu.edu.cn) and Wei Xu (wxu@seu.edu.cn)

This work was supported in part by the National Natural Science Foundation of China under Grant 61571118, Grant 61471114, and Grant 61601115, and in part by the National Science and the Six Talent Peaks Project in Jiangsu Province under Grant GDZB-005.

ABSTRACT The conflict between heavy training overhead and large beamforming gain is a bottleneck to deploy millimeter-wave (mmWave) communications for the next-generation wireless networks. In response, this paper proposes a subarray-cooperation-based multi-resolution codebook design and the corresponding beam alignment scheme, which enables the mmWave backhaul links to quickly align the desired beam pairs under single-dominant-path channels. The proposed codebook is of a hybrid digital/analog structure, in which the digital component selects subarrays and handles the coupling impacts among the selected subarrays, and the analog component shapes essential sub-beams using phase-shifter groups. In particular, the analog beamformers are configured as equal-size discrete Fourier transform vectors, which are easy to implement. The resulting beam alignment method adaptively selects initial layers according to different transmission signal-to-noise ratios, guaranteeing sufficient success ratios on angle detection. The numerical results evaluate the effectiveness of the proposed scheme.

INDEX TERMS Backhaul link, beam alignment/training, millimeter-wave (mmWave), multi-resolution codebook.

I. INTRODUCTION

Millimeter-wave (mmWave) and sub-terahertz (sub-THz) communications are envisioned as promising candidates for future wireless communications owing to the abundant spectrum resource in the range of 30-300 giga-hertz (GHz), which enables giga-bit-per-second (Gbps) data rate in both wireless-local-area-networks (WLANs) and cellular communications [1]–[3]. However, transmissions on such high-frequency band are vulnerable to much more severe path loss than those in microwave band [4]–[7]. To combat the undesired attenuation, directional transmissions with large-scale arrays are crucial to reap large beamforming gain. Thanks to the reduced wavelength in mmWave, more antennas can be arranged in small dimension [8], [9].

With the increasing array scale, however, channel estimation for mmWave communications is challenging due to the extremely large estimation-dimension [10]. The channel estimation methods for traditional multiple-input multiple-output (MIMO) systems are not feasible for mmWave and sub-THz communications any more [11]–[13]. Owing to the sparsity of mmWave and sub-THz channel, only limited multiple path components (MPCs) are required to be considered [14], [15]. There is growing interest in pursuing the solutions to the sparse-channel-estimation problem. Basically, the related works can be organized into the following categories. The first is the compressive-sensing (CS) based channel estimation, which was formulated as a sparsity-reconstruction problem and solved with CS tools in [16] and [17]. The other category is the codebook based switch-beamforming approach, which was also attractive due to the low complexity [18]–[20]. With predefined codebooks, transceivers align their beam-pair by searching for the best codeword combinations, which captures the largest eigenvalue offered by the sparse channel [21]. Straightforwardly, the dominant MPCs can be sounded by exhaustively searching all the codewords in a codeword-wise way. Whereas, the computing cost of such a brute way increases exponentially with the number of codewords, leading to

the unbearable overhead, even in the point-to-point communications.

To reduce searching overhead, initial work was proposed in [22], in which a multi-resolution codebook was devised by deactivating (DEACT) partial antennas. Hur *et al.* [23] improved the performance of the codebook by exploiting the subarray technique. A complete multi-resolution analog codebook was investigated in [24], which jointly leveraged the subarray and the deactivation techniques. References [25] and [26] further developed hybrid codebook designs, in which only two radio-frequency (RF) chains were required. A phase-shifted discrete Fourier transform (PS-DFT) multi-resolution codebook was proposed in [27], which could be easily implemented with the existing hardware [28]. In contrast to the well-investigated codebook designs for pure analog beamforming and hybrid precoding with fully-connected structures, limited works were dedicated to subarray structures due to the difficulty of pursuing flat beam pattern with a few RF chains. Reference [29] presented a multi-resolution codebook design for the mmWave systems with subarray structures, in which the methods of beam-enhancing and beam-broadening were investigated. Moreover, Lin *et al.* [30] studied a multi-resolution codebook design with time-delay line and proposed the corresponding low-complexity implementations.

However, most exiting works on multi-resolution codebook designs for the subarray-structure mmWave systems suffer from either performance degradation due to significant beam fluctuation or high hardware complexity. To tackle these issues, in this paper, we propose a subarray-cooperation-based PS-DFT codebook design and the corresponding beam alignment scheme in the context of frequency-division-duplexing (FDD). The coupling among different subarrays is elegantly handled by a digital beamformer, yielding flat beam patterns. Moreover, RF beamformers are configured as equal-size DFT vectors, leading to simplified hardware implementation. Additionally, the layers for initial searching are adaptively selected under different transmission signal-to-noise ratios (SNRs), guaranteeing sufficient success ratios on angle detection. The main contributions of this paper can be summarized as follows:

- We analyze the phase difference between adjacent DFT vectors' beam gain in the context of *subarray structures*, which reveals that the constructive and destructive interactions between these sub-beams are inevitable.
- We propose a beam scaling strategy comprising beam widening and beam shrinking, both of which are based on multi-subarray cooperations.
- Incorporating the impact of the DFT vectors' phase-difference, we derive phase-shift-coefficients (PSCs) to pursue flat beam pattern for different beam scaling strategies.
- We propose a subarray-cooperation-based multi-resolution codebook design, in which analog components are configured as equal-size DFT vectors and digital components are used to select subarrays and handle the coupling between subarrays.

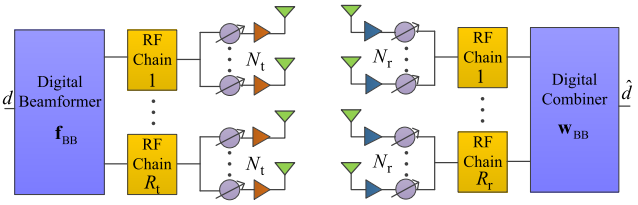

FIGURE 1. System model of mmWave backhaul links with subarray structures.

- With the proposed codebook, we obtain the analytical expression of the received SNR under Rician channel, which is leveraged to adaptively select codebook layers for the initial beam searching under different transmission SNRs.

The rest of this paper is organized as follows: The system model, channel model and problem formulation are described in Section II. In Section III, we investigate a subarray-cooperation-based multi-resolution codebook design. The adaptive beam alignment is then discussed in Section IV. Numerical results are provided in Section V, before concluding this paper in Section VI.

Notation: a, $\mathbf{a}$, $\mathbf{A}$ and $\mathcal{A}$ denote a scalar, a column vector, a matrix, and a set, respectively. For a real-value scalar a, $\lfloor a \rfloor$ and $\lceil a \rceil$ indicate the largest integer less than or equal to a and the smallest integer greater than or equal to a, respectively. For a vector $\mathbf{a}$, $[\mathbf{a}]_i$ is the i-th entry of $\mathbf{a}$, $[\mathbf{a}]_{i:j}$ denotes the vector with elements being $[\mathbf{a}]_i$ to $[\mathbf{a}]_j$, and $\|\mathbf{a}\|_p$ represents the p-norm of $\mathbf{a}$. For a matrix $\mathbf{A}$, $\mathbf{A}^T$ and $\mathbf{A}^H$ represent the transpose and Hermitian transpose of $\mathbf{A}$, respectively. $[\mathbf{A}]_{:,r}$ is the r-th column of $\mathbf{A}$. $[\mathbf{A}]_{n,r}$ is the (n, r)-th element of $\mathbf{A}$. For an $N \times R$ matrix $\mathbf{A}$, diag($\mathbf{A}$) is an $RN \times R$ block diagonal matrix, in which non-zero entries are $[\mathrm{diag}(\mathbf{A})]_{(r-1)N+1:rN,r} = [\mathbf{A}]_{:,r}$, $1 \le r \le R$. For a set $\mathcal{A}$, $|\mathcal{A}|$ denotes the cardinality of set $\mathcal{A}$. Furthermore, $\mathbf{z} \sim \mathcal{CN}(\mathbf{m}, \mathbf{R})$ represents a complex Gaussian vector with mean $\mathbf{m}$ and covariance $\mathbf{R}$. The operators $\odot$ and $\mathbb{E}$ denote Hadamard product and statistical expectation, respectively.

II. SYSTEM DESCRIPTION

In this section, we present the system model considered in this paper, followed by the channel model and problem formulation.

A. SYSTEM MODEL

We consider a point-to-point mmWave backhaul link with subarray structures at both sides. As shown in Fig. 1, the transmitter (receiver) is deployed with R_{t} (R_{r}) RF chains, and each RF chain is exclusively attached to an N_{t}-element (N_{r}-element) uniform-linear-array (ULA) via the corresponding phase-shifter network and power-amplifier group (low-noise-amplifier group).

For downlink transmission, the transmitter conducts an $R_{\mathrm{t}} \times 1$ digital beamformer $\mathbf{f}_{\mathrm{BB}}$ followed by an $R_{\mathrm{t}}N_{\mathrm{t}} \times R_{\mathrm{t}}$ analog beamformer $\mathbf{F}_{\mathrm{RF}}$. Denoting $\mathbf{f}' = \mathbf{F}_{\mathrm{RF}}\mathbf{f}_{\mathrm{BB}}$ as a composite beamformer at the transmitter, the transmitted signal is given by

$$\mathbf{x} = \sqrt{P}\mathbf{f}'d, \tag{1}$$

where d denotes either a pilot symbol during the beam-alignment phase or a data symbol in the data-transmission phase with $\mathbb{E}(|d|^2) = 1$, and P is the total transmission power. To satisfy this total transmission power constraint, $\|\mathbf{f}'\|_2^2 = 1$ should hold. Since each RF chain drives only one *subarray* rather than the whole *array*, $\mathbf{F}_{\mathrm{RF}}$ is a block diagonal matrix [11], i.e.,

$$\begin{aligned}\mathbf{F}_{\mathrm{RF}} &= [\bar{\mathbf{f}}_1^{\mathrm{RF}}, \cdots, \bar{\mathbf{f}}_{R_{\mathrm{t}}}^{\mathrm{RF}}] \\ &= \mathrm{diag}(\mathbf{f}_1^{\mathrm{RF}}, \cdots, \mathbf{f}_{R_{\mathrm{t}}}^{\mathrm{RF}}) \in \mathbb{C}^{R_{\mathrm{t}}N_{\mathrm{t}} \times R_{\mathrm{t}}},\end{aligned} \tag{2}$$

where $\mathbf{f}_r^{\mathrm{RF}} \in \mathbb{C}^{N_{\mathrm{t}} \times 1}$, $1 \le r \le R_{\mathrm{t}}$, is the array weighting vector (AWV) associated with the r-th subarray [29], [30]. Moreover, since $\mathbf{F}_{\mathrm{RF}}$ is implemented with analog phase shifters, the modulus of each non-zero element is constant [16], i.e., $|[\mathbf{F}_{\mathrm{RF}}]_{n,r}|^2 = 1/N_{\mathrm{t}}$.

Within a coherence-time block, the observed signal can be expressed as

$$\mathbf{r} = \sqrt{P}\mathbf{H}\mathbf{f}'d + \mathbf{n}, \tag{3}$$

where $\mathbf{H}$ represents the $R_{\mathrm{r}}N_{\mathrm{r}} \times R_{\mathrm{t}}N_{\mathrm{t}}$ mmWave channel from the transmitter to the receiver, and $\mathbf{n}$ denotes the Gaussian noise vector with power σ_n^2, i.e., $\mathbf{n} \sim \mathcal{CN}(\mathbf{0}, \sigma_n^2\mathbf{I}_{R_{\mathrm{r}}N_{\mathrm{r}}})$ [24].

At the receiver, a unit-power composite combiner $\mathbf{w}'$ comprising an analog combiner $\mathbf{W}_{\mathrm{RF}}$ and a digital combiner $\mathbf{w}_{\mathrm{BB}}$ is applied to combine the observed signal $\mathbf{r}$. Therefore, the received signal can be written as

$$\begin{aligned}y &= \sqrt{P}\mathbf{w}'^H\mathbf{H}\mathbf{f}'d + \mathbf{w}'^H\mathbf{n} \\ &= \sqrt{P}\mathbf{w}_{\mathrm{BB}}^H\mathbf{W}_{\mathrm{RF}}^H\mathbf{H}\mathbf{F}_{\mathrm{RF}}\mathbf{f}_{\mathrm{BB}}d + \mathbf{w}_{\mathrm{BB}}^H\mathbf{W}_{\mathrm{RF}}^H\mathbf{n}.\end{aligned} \tag{4}$$

B. CHANNEL MODEL

Due to the sparsity in mmWave channels, this paper adopts a geometric channel model with L scatters, i.e.,

$$\mathbf{H} = \sqrt{R_{\mathrm{r}}N_{\mathrm{r}}R_{\mathrm{t}}N_{\mathrm{t}}}\sum_{l=1}^{L}\alpha_l\mathbf{a}(R_{\mathrm{r}}N_{\mathrm{r}}, \Phi_l^{\mathrm{r}})\mathbf{a}^H(R_{\mathrm{t}}N_{\mathrm{t}}, \Phi_l^{\mathrm{t}}), \tag{5}$$

where α_l denotes the small-scale fading gain of the l-th path with $\sum_{l=1}^{L}\mathbb{E}(|\alpha_l|^2) = 1$. $\mathbf{a}(R_{\mathrm{t}}N_{\mathrm{t}}, \Phi_l^{\mathrm{t}})$ represents the array response vector (ARV) at the transmitter [24], [25]. When an $(R_{\mathrm{t}}N_{\mathrm{t}})$-element ULA with half-wavelength antenna spacing is adopted, the ARV can be represented as

$$\begin{aligned}&\mathbf{a}\left(R_{\mathrm{t}}N_{\mathrm{t}}, \Phi_l^{\mathrm{t}}\right) \\ &= \frac{1}{\sqrt{R_{\mathrm{t}}N_{\mathrm{t}}}}[1, \cdots, e^{j\pi((r-1)N_{\mathrm{t}}+n-1)\Phi_l^{\mathrm{t}}}, \cdots, e^{j\pi(R_{\mathrm{t}}N_{\mathrm{t}}-1)\Phi_l^{\mathrm{t}}}]^T, \\ &\qquad\qquad \text{for } 1 \le r \le R_{\mathrm{t}},\ 1 \le n \le N_{\mathrm{t}},\end{aligned} \tag{6}$$

where $\Phi_l^{\mathrm{t}} \triangleq \sin\varphi_l^{\mathrm{t}}$, and φ_l^{t} is the physical angle of departure (AoD) at the transmitter. For convenience, AoD refers to Φ_l^{t} in the rest of this paper [24], [27]. At the receiver, $\mathbf{a}(R_{\mathrm{r}}N_{\mathrm{r}}, \Phi_l^{\mathrm{r}})$ and angle of arrival (AoA) have the similar definitions as $\mathbf{a}\left(R_{\mathrm{t}}N_{\mathrm{t}}, \Phi_l^{\mathrm{t}}\right)$ and AoD at the transmitter, respectively.

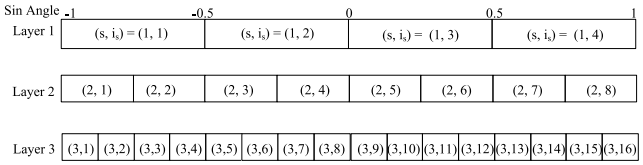

FIGURE 2. An illustration of a radix-2 multi-resolution codebook.

C. PROBLEM FORMULATION

The *received* SNR is defined as

$$\mathrm{SNR} = \frac{P|\mathbf{w}'^H\mathbf{H}\mathbf{f}'|^2}{|\mathbf{w}'^H\mathbf{n}|^2} = \frac{P}{\sigma_n^2}|\mathbf{w}'^H\mathbf{H}\mathbf{f}'|^2, \tag{7}$$

where P/σ_n^2 and $|\mathbf{w}'^H\mathbf{H}\mathbf{f}'|^2$ are the total *transmission* SNR and the power gain, respectively [24]. Our goal is to maximize the effective spectrum efficiency, which is given by

$$R_{\mathrm{e}} = \frac{T - T_{\mathrm{e}}}{T}\mathbb{E}(\log_2(1 + \mathrm{SNR})), \tag{8}$$

where T_{e} and T are the training overhead and the number of time slots within an entire transmission block, respectively.

The composite beamformer $\mathbf{f}'$ (combiner $\mathbf{w}'$) is selected from a composite codebook $\mathcal{F}'$ ($\mathcal{W}'$), which contains an analog component $\mathcal{F}_{\mathrm{RF}}$ ($\mathcal{W}_{\mathrm{RF}}$) and a digital component $\mathcal{F}_{\mathrm{BB}}$ ($\mathcal{W}_{\mathrm{BB}}$). Thus, the problem in this paper can be formulated as

$$\begin{aligned}\max_{\mathbf{F}_{\mathrm{RF}}, \mathbf{f}_{\mathrm{BB}}, \mathbf{W}_{\mathrm{RF}}, \mathbf{w}_{\mathrm{BB}}, T_{\mathrm{e}}}\ & R_{\mathrm{e}} \\ \text{s.t. } & \mathbf{F}_{\mathrm{RF}} \in \bar{\mathcal{F}}_{\mathrm{RF}},\quad \mathbf{f}_{\mathrm{BB}} \in \mathcal{F}_{\mathrm{BB}},\ \|\mathbf{F}_{\mathrm{RF}}\mathbf{f}_{\mathrm{BB}}\|_2^2 = 1, \\ & \mathbf{W}_{\mathrm{RF}} \in \bar{\mathcal{W}}_{\mathrm{RF}},\ \mathbf{w}_{\mathrm{BB}} \in \mathcal{W}_{\mathrm{BB}}, \\ & 0 \le T_{\mathrm{e}} \le T,\end{aligned} \tag{9}$$

where $\bar{\mathcal{F}}_{\mathrm{RF}}$ ($\bar{\mathcal{W}}_{\mathrm{RF}}$) is the block-diagonal form of $\mathcal{F}_{\mathrm{RF}}$ ($\mathcal{W}_{\mathrm{RF}}$).

Solving problem (9) is equivalent to searching for the best beam pairs, ($\mathbf{F}_{\mathrm{RF}}$, $\mathbf{f}_{\mathrm{BB}}$) and ($\mathbf{W}_{\mathrm{RF}}$, $\mathbf{w}_{\mathrm{BB}}$), in the predefined codebooks ($\mathcal{F}_{\mathrm{RF}}$, $\mathcal{F}_{\mathrm{BB}}$) and ($\mathcal{W}_{\mathrm{RF}}$, $\mathcal{W}_{\mathrm{BB}}$) to maximize the received SNR with small overhead. Since the receiver shares the same composite codebook design with the transmitter, we focus on issues at the transmitter, and assume $N_{\mathrm{t}} = N_{\mathrm{r}} = N$ and $R_{\mathrm{t}} = R_{\mathrm{r}} = R$ for concise explanation, where N and R are integer power of 2.

III. SUBARRAY-COOPERATION-BASED MULTI-RESOLUTION CODEBOOK DESIGN

In this section, we first present the hierarchical structure of a radix-2 codebook. A hybrid PS-DFT codebook design is then investigated, which exploits multi-subarray cooperation. The proposed codebook design is finally summarized in Algorithm 1.

A. MULTI-RESOLUTION CODEBOOK STRUCTURE

An S-layer radix-2 codebook is illustrated in Fig. 2. For a given layer s ($1 \le s \le S$), the whole angle domain $\mathcal{D} = [-1, 1)$ is uniformly partitioned into I_s non-overlapped subregions with $B_s = 2/I_s$ angle range in each subregion, such that the i-th subregion in the s-th layer is

$$\begin{aligned}&\mathcal{D}_{(s,i)} = [-1 + (i-1)B_s, -1 + iB_s), \\ &\qquad\qquad \text{for } 1 \le i \le I_s,\ 1 \le s \le S.\end{aligned} \tag{10}$$

Furthermore, the region $\mathcal{D}_{(s,i)}$ is the union of two associated subregions in the $(s+1)$-th layer, i.e.,

$$\mathcal{D}_{(s,i)} = \bigcup_{i'=2i-1}^{2i} \mathcal{D}_{(s+1,i')}, \quad \text{for } 1 \le i \le I_s,\ 1 \le s \le S-1. \tag{11}$$

Accordingly, each subregion $\mathcal{D}_{(s,i)}$ is covered by a dedicated codeword $\mathcal{F}'_{(s,i)}$, the beamwidth of which is B_s. And $\mathcal{F}'_{(s,i)}$ steers along the central angle of $\mathcal{D}_{(s,i)}$, $\Phi_{(s,i)}$. This method can be mathematically depicted as

$$\mathcal{D}_{(s,i)} = \mathcal{CV}(\mathcal{F}'_{(s,i)}) \tag{12}$$

and

$$\Phi_{(s,i)} = -1 + (i-1/2)B_s, \quad \text{for } 1 \le i \le I_s,\ 1 \le s \le S, \tag{13}$$

where $\mathcal{CV}(\mathcal{F}'_{(s,i)})$ represents the angle coverage of $\mathcal{F}'_{(s,i)}$, and $\mathcal{F}'_{(s,i)}$ is the i-th codeword of the s-th layer in the codebook. Moreover, $\mathcal{F}'_{(s,i)}$, termed as a parent-codeword, has two corresponding child-codewords in the $(s+1)$-th layer, $\mathcal{F}'_{(s+1,i')}$, i.e.,

$$\mathcal{CV}(\mathcal{F}'_{(s,i)}) = \bigcup_{i'=2i-1}^{2i} \mathcal{CV}(\mathcal{F}'_{(s+1,i')}), \quad \text{for } 1 \le i \le I_s,\ 1 \le s \le S-1. \tag{14}$$

B. SUBARRAY-COOPERATION-BASED HYBRID CODEBOOK DESIGN

In this subsection, we investigate a beam scaling strategy, followed by the construction of the first composite codeword for a given layer. Other codewords in the fixed layer are then obtained by beam rotation.

1) BEAM SCALING STRATEGY

For a given-scale *array*, on one hand, beam pattern can be straightforwardly widened by turning off partial *subarrays*, while considerable RF chains are required. On the other hand, as illustrated in Fig. 2 and (14), the coverage of a parent-codeword is the union of that of the corresponding child-codewords. It is natural that a synthesized beam can be *further* widened with multiple narrow beams. Accordingly, the desired codeword in a relatively low layer can also be constructed by appropriately combining the codewords in a relatively high layer. To demonstrate this idea, we consider the complete beam gain $G(\mathbf{f}', \Phi)$:

$$\begin{aligned} & G(\mathbf{f}', \Phi) \\ & \overset{(a)}{=} \sqrt{RN}\mathbf{a}^H(RN, \Phi)\mathbf{f}' \\ & \overset{(b)}{=} \sqrt{RN}\mathbf{a}^H(RN, \Phi)\sum_{r=1}^{R}[\mathbf{f}_{\mathrm{BB}}]_r[\mathbf{F}_{\mathrm{RF}}]_{:,r} \\ & \overset{(c)}{=} \sqrt{RN}\sum_{r=1}^{R}[\mathbf{f}_{\mathrm{BB}}]_r e^{-j\pi(r-1)N\Phi}\frac{\sqrt{N}}{\sqrt{RN}}\mathbf{a}^H(N, \Phi)\mathbf{f}_r^{\mathrm{RF}} \\ & = \sum_{r=1}^{R}[\mathbf{f}_{\mathrm{BB}}]_r e^{-j\pi(r-1)N\Phi}\sqrt{N}\mathbf{a}^H(N, \Phi)\mathbf{f}_r^{\mathrm{RF}} \\ & \overset{(d)}{=} \sum_{r=1}^{R}[\mathbf{f}_{\mathrm{BB}}]_r e^{-j\pi(r-1)N\Phi}G(\mathbf{f}_r^{\mathrm{RF}}, \Phi), \end{aligned} \tag{15}$$

where (a) and (d) follow form the definition of beam gain, (b) comes from $\mathbf{f}' = \mathbf{F}_{\mathrm{RF}}\mathbf{f}_{\mathrm{BB}}$ in the system model, (c) leverages the results in (2) and (6).

Equation (15) reveals that the complete beam gain is the linear combination of multiple sub-beams' beam gain, and each sub-beam is weighted by the factor of $[\mathbf{f}_{\mathrm{BB}}]_r e^{-j\pi(r-1)N\Phi}$. This insight motivates us that the desired beam with wide beamwidth can be synthesized with the multiple narrow sub-beams. To realize this, candidate sub-beams are scheduled to steer to different angles with appropriate angle intervals, such that the coverage of the desired beam is perfectly occupied. Specifically, the desired beam is synthesized with multiple unitary sub-beams shaped by different subarrays, and the synthesis of candidate sub-beams is achieved by multiple-subarray cooperation. Thanks to the subarray structure, this cooperation among different subarrays can be readily realized via adjusting $[\mathbf{f}_{\mathrm{BB}}]_r$.

To illustrate the insights behind multiple-subarray cooperation, we take the following case as an example: The number of subarrays is $R = 2$ and each subarray has $N = 8$ antennas. Each 8-element subarray is used to establish unitary sub-beam with $2/8$ beamwidth. When these sub-beams steer along the same direction, the beamwidth of the synthesized beam may be $2/16$; Whereas, when the sub-beams steer to different angles with $2/8$ interval, the resultant beam's beamwidth yields $4/8$. The former cooperation between subarrays is termed as *Beam Shrinking*, and the latter cooperation is called *Beam Widening*.

2) THE FIRST COMPOSITE CODEWORD DESIGN

In this subsection, we focus on constructing the first composite codeword $\mathcal{F}'_{(s,1)}$ of the s-th layer, which consists of an analog codeword $\mathcal{F}_{\mathrm{RF}(s,1)}$ and a digital codeword $\mathcal{F}_{\mathrm{BB}(s,1)}$. For concise notation, we drop the index of the i-th codeword.

a: THE FIRST ANALOG CODEWORD DESIGN

Inspired by the aforementioned beam scaling strategy, the desired beam pattern of $\mathbf{f}'_{(s,1)}$ in (15) can be synthesized by beam widening or beam shrinking with $\hat{R}_s$ candidate subarrays, each of which is used to shape a unitary sub-beam $G(\mathbf{f}_r^{\mathrm{RF}}, \Phi)$. For the r-th subarray, to reap the largest beam gain along the cental angle Φ_r, its AWV should be configured in an ARV fashion, i.e., $\mathbf{f}_r^{\mathrm{RF}} = \mathbf{a}(N, \Phi_r)$. Under this configuration, the beam gain of the r-th beamformer is

$$\begin{aligned} & G(\mathbf{f}_r^{\mathrm{RF}}, \Phi)\,|_{\mathbf{f}_r^{\mathrm{RF}}=\mathbf{a}(N,\Phi_r)} \\ & \overset{(a)}{=} \sqrt{N}\mathbf{a}^H(N, \Phi)\mathbf{f}_r^{\mathrm{RF}}\,|_{\mathbf{f}_r^{\mathrm{RF}}=\mathbf{a}(N,\Phi_r)} \\ & \overset{(b)}{=} \frac{1}{\sqrt{N}}\sum_{n=1}^{N} e^{-j\pi(n-1)(\Phi-\Phi_r)} \\ & \overset{(c)}{=} \frac{1}{\sqrt{N}}\frac{\sin[\pi N(\Phi-\Phi_r)/2]}{\sin[\pi(\Phi-\Phi_r)/2]}e^{[-j\pi(N-1)(\Phi-\Phi_r)/2]}, \end{aligned} \tag{16}$$

where (a) follows from the definition of beam gain, (b) comes from the definition of ARV in (6), and (c) holds due to the sum of geometric sequence. The magnitude of $G(\mathbf{f}_r^{\mathrm{RF}}, \Phi)$ has the following properties:

P.1: $|G(\mathbf{f}_r^{\mathrm{RF}}, \Phi)|$ is an even function of Φ at Φ_r;

P.2: The maximum of $|G(\mathbf{f}_r^{\mathrm{RF}}, \Phi)|$ is $|G(\mathbf{f}_r^{\mathrm{RF}}, \Phi_r)| = \sqrt{N}$, and $|G(\mathbf{f}_r^{\mathrm{RF}}, \Phi)|_{\Phi=\Phi_r\mp\frac{1}{N}} = \frac{1}{\sqrt{N}\sin(\pi/2N)} \approx \frac{2\sqrt{N}}{\pi} \approx 0.6366\sqrt{N}$;

P.3: The envelope of $|G(\mathbf{f}_r^{\mathrm{RF}}, \Phi)|$, $1/\{\sqrt{N}|\sin[\pi(\Phi-\Phi_r)/2]|\}$, is increasing on $[-1+\Phi_r, \Phi_r)$ and decreasing on $[\Phi_r, \Phi_r+1)$;

P.4: The period of the nominator of $|G(\mathbf{f}_r^{\mathrm{RF}}, \Phi)|$ is $2/N$.

From P.4, the angle spacing between adjacent sub-beams, $\underline{B}$, should be integer multiples of $2/N$. Meanwhile, P.3 and P.2 require $\underline{B} \leq 2/N$, otherwise, beam sinks will occur. Consequently, we have the following proposition.

Proposition 1: When $\hat{R}_s$ consecutive subarrays are selected to conduct beam widening, the angle spacing between adjacent sub-beams, $\underline{B}$, should be $2/N$, such that

$$\Phi_{s,r} = -1 + (r-1/2)\underline{B} = -1 + (2r-1)/N, \quad \text{for } 1 \leq r \leq \hat{R}_s. \tag{17}$$

From (16), P.2 and P.4, it can be observed that the beamwidth $2/N$ is in reverse proportion to the scale of array. Hence, we have the following proposition.

Proposition 2: The beam shrinkage of $1/\hat{R}_s$ can be realized by $\hat{R}_s$-consecutive-subarray cooperation, where all the AWVs of these subarrays steer along the same direction, i.e.,

$$\Phi_{s,r} = -1 + \underline{B}/(2\hat{R}_s) = -1 + 1/(\hat{R}_s N), \quad \text{for } 1 \leq r \leq \hat{R}_s. \tag{18}$$

Thus, the first analog codeword of the s-th layer can be designed as

$$[\mathcal{F}_{\mathrm{RF}(s,1)}]_{:,r} = \mathbf{a}(N, \Phi_{s,r}), \quad \text{for } 1 \leq r \leq \hat{R}_s. \tag{19}$$

It is noted that, the AWV on the quantized angles $\{\Phi_{s,r}\}$ in (19) yields a generalized N-point DFT vector with $-(1+N)/2$ offset [27]. Since the AWVs for all the selected subarrays are configured as the equal-length (N-element) DFT vectors, the hardware implementation will be simplified.

b: THE FIRST DIGITAL CODEWORD DESIGN

With the candidate sub-beams shaped by multiple subarrays, the digital codeword is used to select these subarrays and combine the associated sub-beams to approach the desired beam pattern.

For an R-subarray transmitter, the number of layers in a radix-2 codebook is $S = 2\lfloor \log_2 R \rfloor + 1$. Note that, the method of multi-subarray cooperation in the first half layers is beam widening, while beam-shrinking cooperation occurs in the last half layers. To respect these different cooperations, we define a broaden factor as $\mu_s = 2^{[(\lfloor \log_2 R \rfloor + 1) - s]}$, which is the ratio of the beamwidth of a codeword in the s-th layer to that of a codeword in the $(\lfloor \log_2 R \rfloor + 1)$-th layer. It is clear that $\mu_s \geq 1$ corresponds to beam widening and $\mu_s < 1$ is associated with beam shrinking. With the broaden

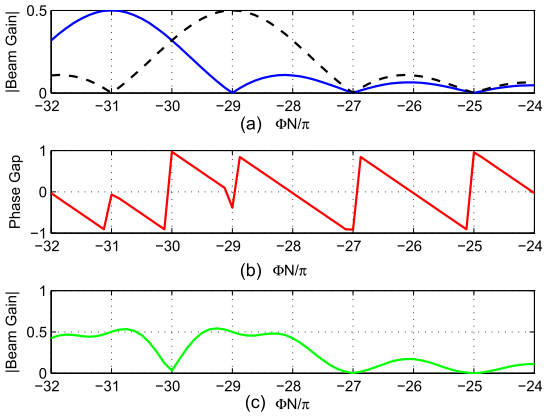

FIGURE 3. An example of phase difference between adjacent sub-beams, in which $R = 2$, $N = 32$.

factor μ_s, the number of subarrays required to shape sub-beams is

$$\hat{R}_s = \begin{cases} \mu_s, & \text{for } \mu_s \geq 1, \\ 1/\mu_s, & \text{for } \mu_s < 1. \end{cases} \tag{20}$$

Incorporating the total transmit power constraint, the first digital codeword of the s-th layer can be designed as

$$\mathcal{F}_{\mathrm{BB}(s,1)} = \begin{cases} \frac{1}{\sqrt{\hat{R}_s}}[e^{j\theta_1}, \cdots, e^{j\theta_{\hat{R}_s}}, \ [\mathbf{0}]_{1\times(R-\hat{R}_s)}]^T, & \text{for } \mu_s \geq 1, \\ \frac{1}{\sqrt{\hat{R}_s}}[e^{j\theta'_1}, \cdots, e^{j\theta'_{\hat{R}_s}}, \ [\mathbf{0}]_{1\times(R-\hat{R}_s)}]^T, & \text{for } \mu_s < 1, \end{cases} \tag{21}$$

where θ_r (θ'_r) is the phase-shift-coefficient (PSC) for the r-th subarray.

Note that the determination of PSCs is vital to pursue flat beam pattern and reap large beam gain. As depicted in Fig. 3, the sub-figure (a) provides two sub-beams, which are shaped by two consecutive 32-element subarrays. Sub-figure (b) plots the phase difference between these sub-beams. From the sub-figure (c), it can be observed that the resulting beam is far away from the desired beam, which should flatly cover the angle range of $[-32, -28)$. The rest of this subsection will focus on determining PSCs to pursue flat beam pattern.

When multiple N-point DFT AWVs are cooperatively used to synthesize the desired beam, the complete beam gain in (15) can be rewritten as

$$\begin{aligned} G(\mathbf{f}'_s, \Phi) \ |_{\mathbf{f}_{s,r}^{\mathrm{RF}}=\mathbf{a}(N,\Phi_{s,r})} &\overset{(a)}{=} \sum_{r=1}^{\hat{R}_s} [\mathbf{f}_{\mathrm{BB}(s)}]_r e^{-j\pi(r-1)N\Phi} G(\mathbf{f}_{s,r}^{\mathrm{RF}}, \Phi) \ |_{\mathbf{f}_{s,r}^{\mathrm{RF}}=\mathbf{a}(N,\Phi_{s,r})} \\ &\overset{(b)}{=} \sum_{r=1}^{\hat{R}_s} \frac{[\mathbf{f}_{\mathrm{BB}(s)}]_r}{\sqrt{N}} \frac{\sin[\pi N(\Phi-\Phi_{s,r})/2]}{\sin[\pi(\Phi-\Phi_{s,r})/2]} \\ &\quad \times e^{\{-j\pi[(r-1)N\Phi+(N-1)(\Phi-\Phi_{s,r})/2]\}} \\ &\overset{(c)}{=} \sum_{r=1}^{\hat{R}_s} \frac{1}{\sqrt{\hat{R}_s N}} \frac{\sin[\pi N(\Phi-\Phi_{s,r})/2]}{\sin[\pi(\Phi-\Phi_{s,r})/2]} \\ &\quad \times e^{\{-j\pi[(r-1)N\Phi+(N-1)(\Phi-\Phi_{s,r})/2]+j\theta_r\}}, \end{aligned} \tag{22}$$

where (a), (b) and (c) follow from the results in (15), (16) and (21), respectively. From (22), it can be found that the beam gain of the r-th sub-beam is weighted by a phase-only term $e^{[-j\pi(r-1)N\Phi]}$ before linearly combined with other sub-beams, which is induced by the wave-path difference between different subarrays. Moreover, *the phase of the phase weighting term is a linear function of angle Φ, which leads to spatial-frequency-selective-fading*. This fading will bring different impacts for different multi-subarray-cooperation categories.

i) PSC DETERMINATION BASED ON FADING IMPACT FOR BEAM WIDENING COOPERATION

When $\Phi_{s,r}$ in (22) follows from (17), the resultant beam gain at $\Phi_{s,r}$, $|G(\mathbf{f}_s', \Phi_{s,r})|$, is $\sqrt{N/\hat{R}_s}$. For ideal beam pattern, the magnitude of $G(\mathbf{f}_s', \Phi)$ at other angles in the coverage of the desired beam should also be $\sqrt{N/\hat{R}_s}$. Owing to the spatial-frequency-selective-fading, the beam gain of different sub-beams adds constructively on some angle ranges and destructively at other angles. Specifically, according to P.1, the worst case may occur at the intersections between adjacent sub-beams, which are located at

$$\tilde{\Phi}_{s,r} = -1 + (r-1)\underline{B} = -1 + 2(r-1)/N, \quad \text{for } 1 < r \le \hat{R}_s. \tag{23}$$

Since two adjacent sub-beams have the same beam-gain magnitude at the intersection point $\tilde{\Phi}_{s,r}$, the null point of $G(\mathbf{f}_s', \tilde{\Phi}_{s,r})$ will occur once the phases of them are reverse. Incorporating P.1 and P.2, we establish the following proposition.

Proposition 3: To construct the first codeword of the s-th layer by exploiting the beam widening cooperation, the PSC of the r-th subarray, θ_r, should be set as

$$\theta_r = r\Delta\theta = -r(N-1)\pi/N, \quad \textit{for } 1 \le r \le \hat{R}_s,\ \mu \ge 1, \tag{24}$$

such that the superposition of the $(r-1)$-th sub-beam and the r-th sub-beam is constructive at their intersection $\tilde{\Phi}_{s,r}$, and destructive at $\tilde{\Phi}_{s,r} \pm 1/N$.

The proof of Proposition 3 is provided in Appendix.

ii) PSC DETERMINATION BASED ON FADING IMPACT FOR BEAM SHRINKING COOPERATION

Different from the beam widening case, in the beam shrinking case, we aim to obtain the same beam pattern of $(\hat{R}_s N)$-element array with $\hat{R}_s$ physically-separated N-element subarrays. To achieve this goal, we have the following proposition.

Proposition 4: To construct the first codeword of the s-th layer by exploiting the beam shrinking cooperation, the PSC of the r-th subarray, θ_r', should be configured as

$$\theta_r' = (r-1)\pi/\hat{R}_s, \quad \text{for } 1 \le r \le \hat{R}_s,\ \mu < 1. \tag{25}$$

Proof: The ARV-fashion AWV of an $(\hat{R}_s N)$-element array is

$$\begin{aligned}
&[\mathbf{f}^{\mathrm{RF}}_{\hat{R}_s N\times 1}]_{(r-1)N+1\,:\,rN} \\
&\overset{(a)}{=} [\mathbf{a}(\hat{R}_s N, \Phi_s)]_{(r-1)N+1\,:\,rN} \\
&\overset{(b)}{=} \frac{1}{\sqrt{\hat{R}_s N}} e^{j\pi(r-1)N\Phi_s}[1, \cdots, e^{j\pi(n-1)\Phi_s}, \cdots, e^{j\pi(N-1)\Phi_s}]^T \\
&\overset{(c)}{=} \frac{1}{\sqrt{\hat{R}_s}} e^{j\pi(r-1)N\Phi_s}\mathbf{a}(N, \Phi_s) \\
&\overset{(d)}{=} \frac{1}{\sqrt{\hat{R}_s}} e^{j\pi(r-1)N\Phi_s}\mathbf{f}^{\mathrm{RF}}_{s,r} \\
&\overset{(e)}{\rightarrow} \theta_r' = (r-1)N\pi\Phi_s \overset{(f)}{=} (r-1)N\pi[-1 + 1/(\hat{R}_s N)] \\
&\overset{(g)}{\rightarrow} \theta_r' = (r-1)\pi/\hat{R}_s,
\end{aligned} \tag{26}$$

where (a) and (d) hold for $\mathbf{f}^{\mathrm{RF}}_{\hat{R}_s N\times 1}$ and $\mathbf{f}^{\mathrm{RF}}_{s,r}$ configured in ARV fashion, respectively. (b) and (c) follow from the ARV definitions of an $(\hat{R}_s N)$-element and an N-element array, respectively. (e) comes from the comparison between (d) and the case of $\mu < 1$ in (21). (f) is obtained by using the result of (18) in Proposition 2. (g) leverages the facts that r is a positive integer and N is an even number. ■

3) BEAM ROTATION

For a given layer s, with the first composite codeword $\mathcal{F}'_{(s,1)}$, any other codeword $\mathcal{F}'_{(s,i)}$, $i > 1$, can be obtained by beam rotation, which is given by

$$\mathcal{F}'_{(s,i)} = \mathrm{diag}(\mathcal{F}_{\mathrm{RF}(s,i)})\,\mathcal{F}_{\mathrm{BB}(s,i)}, \tag{27}$$

in which the analog component of the (s,i)-th codeword is

$$[\mathcal{F}_{\mathrm{RF}(s,i)}]_{:,r} = [\mathcal{F}_{\mathrm{RF}(s,1)}]_{:,r} \odot \sqrt{N}\mathbf{a}(N, (i-1)B_s), \tag{28}$$

where $B_s = \mu_s\underline{B} = 2\mu_s/N$ is the bandwidth of each codeword at the s-th layer. The digital component of the (s,i)-th codeword is

$$\mathcal{F}_{\mathrm{BB}(s,i)} = \begin{cases} \mathcal{F}_{\mathrm{BB}(s,1)}, & \text{for } \mu \ge 1, \\ \mathcal{F}_{\mathrm{BB}(s,1)} \odot \sqrt{R}\mathbf{a}(R, (i-1)NB_s), & \text{for } \mu < 1. \end{cases} \tag{29}$$

It is noted that $\mathcal{F}_{\mathrm{BB}(s,i)}$ is independent of the codeword index i in the given layer when μ is no less than 1. However, when the cooperation between multiple subarrays is beam shrinking (i.e., $\mu < 1$), the digital component $\mathcal{F}_{\mathrm{BB}(s,i)}$ is a function of variables i and r. This conclusion can be drawn from step (d) in (26).

C. PROPOSED CODEBOOK GENERATION ALGORITHM

Until now, we have designed the hybrid codebook $\mathcal{F}'$, which can be summarized in Algorithm 1. Input parameters, N and R, are the number of antennas and RF chains, respectively. For given RF chains R, the radix-2 codebook of

Algorithm 1 Proposed Codebook Generation Algorithm

Input: N, R
Output: $\mathcal{F}_{\mathrm{BB}}, \mathcal{F}_{\mathrm{RF}}$
1 **Initialize:** $S = 2\lfloor \log_2 R \rfloor + 1$, $\mathcal{F}_{\mathrm{BB}} \leftarrow [\mathbf{0}]_{S\times R\times RN}$, and $\mathcal{F}_{\mathrm{RF}} \leftarrow [\mathbf{0}]_{S\times RN\times N\times R}$;
2 **Generate codewords in the s-th layer:**
3 **for** $s = 1 : S$ **do**
4 Compute $\mu_s = 2^{[(\lfloor \log_2 R \rfloor + 1) - s]}$, $B_s = 2\mu_s/N$, $I_s = 2/B_s$;
5 **if** $\mu_s \geq 1$ **then**
6 $\hat{R}_s = \mu_s$;
7 **for** $r = 1 : \hat{R}_s$ **do**
8 $[\mathcal{F}_{\mathrm{RF}}]_{s,1,:,r} = \mathbf{a}(N, -1 + (2r-1)/N)$;
9 $[\mathcal{F}_{\mathrm{BB}}]_{s,r,1} = 1/\sqrt{\hat{R}_s} e^{-jr(N-1)\pi/N}$;
10 **else**
11 $\hat{R}_s = 1/\mu_s$;
12 **for** $r = 1 : \hat{R}_s$ **do**
13 $[\mathcal{F}_{\mathrm{RF}}]_{s,1,:,r} = \mathbf{a}(N, -1 + 1/(\hat{R}_s N))$;
14 $[\mathcal{F}_{\mathrm{BB}}]_{s,r,1} = 1/\sqrt{\hat{R}_s} e^{j(r-1)\pi/\hat{R}_s}$;
15 **for** $i = 1 : I_s$ **do**
16 **for** $r = 1 : \hat{R}_s$ **do**
17 Obtain $[\mathcal{F}_{\mathrm{RF}}]_{s,i,:,r}$ by using (28);
18 **if** $\mu_s \geq 1$ **then**
19 $[\mathcal{F}_{\mathrm{BB}}]_{s,:,i} = [\mathcal{F}_{\mathrm{BB}}]_{s,:,1}$;
20 **else**
21 $[\mathcal{F}_{\mathrm{BB}}]_{s,:,i}$
22 $= [\mathcal{F}_{\mathrm{BB}}]_{s,:,1} \odot \sqrt{R}\mathbf{a}(R, (i-1)NB_s)$;
23 **Return** $\mathcal{F}_{\mathrm{BB}}, \mathcal{F}_{\mathrm{RF}}$;

$S = 2\lfloor \log_2 R \rfloor + 1$ layers can be established. Output is the composite codebook $\mathcal{F}'$, which is composed of the digital codebook $\mathcal{F}_{\mathrm{BB}}$ and the analog codebook $\mathcal{F}_{\mathrm{RF}}$. The digital codebook is an $S \times R \times RN$ three-dimensional matrix, in which the first and the last subscripts denote a layer index and a codeword index in the fixed layer, respectively. The analog codebook is an $S \times RN \times N \times R$ four-dimensional matrix, in which the first two subscripts correspond to a layer index and a codeword index in the fixed layer, respectively.

For the s-th layer, the beam broaden factor μ_s is $\mu_s = 2^{[(\lfloor \log_2 R \rfloor + 1) - s]}$, the beamwidth of each codeword is $2\mu_s/N$, and the total number of codewords is $2/B_s$. The pseudo-code between the 5-th line and the 14-th line in Algorithm 1 is used to construct the first composite codeword for the s-th layer, in which the contents from the 6-th line to the 9-th line correspond to the case of beam widening cooperation, while the lines between 11 and 14 are associated with beam shrinking. The pseudo-instruction between the 15-th line and the 22-th line is developed to obtain other codewords in the s-th layer by beam rotation.

IV. SUBARRAY-BASED COOPERATIVE BEAM ALIGNMENT

In this section, we first present a three-phase beam alignment framework. The subarray-based cooperative beam alignment design is then summarized in an algorithm. Finally, the overhead of the proposed beam alignment scheme is analyzed.

A. THREE-PHASE BEAM ALIGNMENT FRAMEWORK

The proposed beam alignment is composed of three phases: an initial setup phase, the hierarchical beam searching at the transmitter, and the hierarchical beam searching at the receiver.

1) EXHAUSTIVE BEAM SEARCHING IN THE INITIAL SETUP PHASE

Considering limited beamforming gain offered by a wide beam and only a few codewords required to be searched in the initial stage, the transmitter sequentially scans its angle support $\mathcal{D}^{\mathrm{t}}_{\mathrm{AS}} = [\Phi^{\mathrm{t}}_{\mathrm{AS,min}}, \Phi^{\mathrm{t}}_{\mathrm{AS,max}})$, which can be covered with the codewords of the s_{I}-th layer for the initial searching, i.e.,

$$\begin{aligned} -1 + (i^{\mathrm{t}}_{\min} - 1)B^{\mathrm{t}}_{s_{\mathrm{I}}} &\leq \Phi^{\mathrm{t}}_{\mathrm{AS,min}} < -1 + i^{\mathrm{t}}_{\min} B^{\mathrm{t}}_{s_{\mathrm{I}}}, \\ -1 + (i^{\mathrm{t}}_{\max} - 1)B^{\mathrm{t}}_{s_{\mathrm{I}}} &\leq \Phi^{\mathrm{t}}_{\mathrm{AS,max}} < -1 + i^{\mathrm{t}}_{\max} B^{\mathrm{t}}_{s_{\mathrm{I}}}, \end{aligned} \tag{30}$$

where $i^{\mathrm{t}}_{\min}$ and $i^{\mathrm{t}}_{\max}$ are the minimal and maximal index of the corresponding codewords in the s_{I}-th layer to cover $\mathcal{D}^{\mathrm{t}}_{\mathrm{AS}}$, respectively, and $B^{\mathrm{t}}_{s_{\mathrm{I}}}$ is the beamwidth of each codeword at the s_{I}-th layer. It is clear that (30) is equivalent to

$$\begin{aligned} i^{\mathrm{t}}_{\min} &= \lfloor \frac{\Phi^{\mathrm{t}}_{\mathrm{AS,min}} + 1}{B^{\mathrm{t}}_{s_{\mathrm{I}}}} \rfloor + 1, \\ i^{\mathrm{t}}_{\max} &= \lceil \frac{\Phi^{\mathrm{t}}_{\mathrm{AS,max}} + 1}{B^{\mathrm{t}}_{s_{\mathrm{I}}}} \rceil. \end{aligned} \tag{31}$$

Therefore, we have

$$|\mathcal{I}^{\mathrm{t}}_{\mathrm{AS}}(s_{\mathrm{I}})| = i^{\mathrm{t}}_{\max} - i^{\mathrm{t}}_{\min} + 1, \tag{32}$$

where $|\mathcal{I}^{\mathrm{t}}_{\mathrm{AS}}(s_{\mathrm{I}})|$ is the number of codewords required to cover the angle supports $\mathcal{D}^{\mathrm{t}}_{\mathrm{AS}}$ in the s_{I}-th layer.

Similarly, we have $i^{\mathrm{r}}_{\min}$, $i^{\mathrm{r}}_{\max}$ and $|\mathcal{I}^{\mathrm{r}}_{\mathrm{AS}}(s_{\mathrm{I}})|$ at the receiver. For each transmitted codeword, the receiver exhaustively sounds all possible directions in its angle support with $|\mathcal{I}^{\mathrm{r}}_{\mathrm{AS}}(s_{\mathrm{I}})|$ codewords.

2) HIERARCHICAL BEAM SEARCHING IN THE REMAINING PHASE

Once accomplishing the initial setup phase, the receiver combines the received signals in a directional way with the best codeword found in the initial phase. Meanwhile, the transmitter conducts hierarchical beam searching in a binary-tree fashion to obtain the best codeword, which corresponds to the maximal received signal power.

Finally, the transmitter fixes the directional beam with the best codeword found in the second phase, and the dominant path can be extracted by the hierarchial beam searching at the receiver.

B. COOPERATIVE BEAM ALIGNMENT DESIGN UNDER RICIAN FADING CHANNELS

1) TRADEOFF BETWEEN TRANSMISSION SNR AND TRANSCEIVER GAIN

Under Rician fading channels, the received signal in (4) can be rewritten as

$$\begin{aligned} y &\approx \sqrt{P}\mathcal{W}'^{H}_{(s_\mathrm{r},i_\mathrm{r})}\mathbf{H}\mathcal{F}'_{(s_\mathrm{t},i_\mathrm{t})}d+\mathcal{W}'^{H}_{(s_\mathrm{r},i_\mathrm{r})}\mathbf{n}|_{\alpha_l=\alpha_{\mathrm{LS}},\ \Phi^{\mathrm{t}}_l=\Phi^{\mathrm{t}}_{\mathrm{LS}},\ \Phi^{\mathrm{r}}_l=\Phi^{\mathrm{r}}_{\mathrm{LS}}} \\ &\overset{(a)}{=} \sqrt{P}\sqrt{R_\mathrm{r}N_\mathrm{r}}\mathcal{W}'^{H}_{(s_\mathrm{r},i_\mathrm{r})}\mathbf{a}(R_\mathrm{r}N_\mathrm{r},\Phi^{\mathrm{r}}_{\mathrm{LS}})\alpha_{\mathrm{LS}} \\ &\quad\times\sqrt{R_\mathrm{t}N_\mathrm{t}}\mathbf{a}^H(R_\mathrm{t}N_\mathrm{t},\Phi^{\mathrm{t}}_{\mathrm{LS}})\mathcal{F}'_{(s_\mathrm{t},i_\mathrm{t})}d+n. \\ &\overset{(b)}{=} \sqrt{P}G^H(\mathcal{W}'_{(s_\mathrm{r},i_\mathrm{r})},\Phi^{\mathrm{r}}_{\mathrm{LS}})\alpha_{\mathrm{LS}}G(\mathcal{F}'_{(s_\mathrm{t},i_\mathrm{t})},\Phi^{\mathrm{t}}_{\mathrm{LS}})d+n, \end{aligned} \tag{33}$$

where $\mathcal{W}'$ and $\mathcal{F}'$ are the composite codebooks adopted at the receiver and transmitter, respectively. The subscript pairs $(s_\mathrm{r}, i_\mathrm{r})$ and $(s_\mathrm{t}, i_\mathrm{t})$ are the indices of codewords selected from $\mathcal{W}'$ and $\mathcal{F}'$, respectively. α_{LS}, $\Phi^{\mathrm{t}}_{\mathrm{LS}}$ and $\Phi^{\mathrm{r}}_{\mathrm{LS}}$ are the path gain, AoD and AoA of the line-of-sight (LoS) path, respectively. (a) follows from the channel model in (5). (b) comes from the definition of beam gain in (15). Therefore, the received SNR η is given by

$$\eta=\frac{P}{\sigma^2_\mathrm{n}}|\alpha_{\mathrm{LS}}|^2|G(\mathcal{W}'_{(s_\mathrm{r},i_\mathrm{r})},\Phi^{\mathrm{r}}_{\mathrm{LS}})|^2|G(\mathcal{F}'_{(s_\mathrm{t},i_\mathrm{t})},\Phi^{\mathrm{t}}_{\mathrm{LS}})|^2, \tag{34}$$

which is jointly dependent on the transmission SNR P/σ^2_n, path gain $|\alpha_{\mathrm{LS}}|^2$, beamforming gain $|G(\mathcal{F}'_{(s_\mathrm{t},i_\mathrm{t})},\Phi^{\mathrm{t}}_{\mathrm{LS}})|^2$ and combining gain $|G(\mathcal{W}'_{(s_\mathrm{r},i_\mathrm{r})},\Phi^{\mathrm{r}}_{\mathrm{LS}})|^2$.

As mentioned in Section III B, $|G(\mathcal{F}'_{(s,i)},\Phi)|$ should be $\sqrt{N/\mu_s}$ within $\mathcal{CV}(\mathcal{F}'_{(s,i)})$. With the ideal beam patterns at the transceiver, the received SNR can be further approximated as

$$\begin{aligned} \eta^\star &= \frac{P}{\sigma^2_\mathrm{n}}|\alpha_{\mathrm{LS}}|^2|\sqrt{N_\mathrm{r}/\mu_{s_\mathrm{r}}}|^2|\sqrt{N_\mathrm{t}/\mu_{s_\mathrm{t}}}|^2 \\ &= \frac{P}{\sigma^2_\mathrm{n}}|\alpha_{\mathrm{LS}}|^2\frac{N_\mathrm{r}N_\mathrm{t}}{\mu_{s_\mathrm{r}}\mu_{s_\mathrm{t}}} \\ &\overset{(a)}{\to} \frac{P}{\sigma^2_\mathrm{n}}|\alpha_{\mathrm{LS}}|^2(\frac{N}{R})^2 4^{(s-1)}, \end{aligned} \tag{35}$$

where (a) holds when $N_\mathrm{r}=N_\mathrm{t}=N$ and $\mu_{s_\mathrm{r}}=\mu_{s_\mathrm{t}}=\mu_s=2R/2^s$. For a given transceiver and transmission SNR, it can be observed from equation (35) that the received SNR $\eta^\star$ under Rician channels is approximately predictable, which is a single-variable function of s. Moreover, $\eta^\star$ grows exponentially with the codebook-layer index s for beam training. In other words, for a given channel realization, constant $\eta^\star$ could be maintained by using large transceiver gain $(N/R)^2 4^{(s-1)}$ to compensate small P/σ^2_n. Therefore, we have

Remark 1: For a given mmWave Rician channel, the received SNR $\eta^\star$ can be maintained as a constant number by making a tradeoff between the transmission SNR P/σ_n^2 and the training layer s.

2) DETERMINING THE LAYER INDEX FOR INITIAL SEARCHING

The directional transmissions in mmWave backhaul links highly depend on the angle detection ratio, which is further dependent of the received SNR η. Inspired by Remark 1, small transmission SNR should be compensated by choosing large s, such that sufficient $\eta^\star$ can be established during the beam training. Specifically, for hierarchical beam alignment, the received SNR η in the initial phase is commonly small due to the large coverage of low layers' codewords. Thus, we have the following proposition.

Proposition 5: To guarantee some angle detection ratio in the initial beam searching, $\eta^\star$ should be no less than the threshold of $\gamma=(-\ln(P_{\mathrm{FA}}))^2$ [27], where P_{FA} is a given false-alarm probability, i.e., $\eta^\star=\frac{P}{\sigma^2_\mathrm{n}}|\alpha_{\mathrm{LS}}|^2(\frac{N}{R})^2 4^{(s_\mathrm{I}-1)}\geq\gamma=(-\ln(P_{\mathrm{FA}}))^2$.

Thus, the layer index for the initial beam searching is

$$s_\mathrm{I}=\lceil\log_4\frac{\ln^2(P_{\mathrm{FA}})}{(P/\sigma^2_\mathrm{n})|\alpha_{\mathrm{LS}}|^2(N/R)^2}\rceil+1. \tag{36}$$

3) PROPOSED BEAM ALIGNMENT ALGORITHM

With the hybrid codebooks $(\mathcal{F}_{\mathrm{RF}},\ \mathcal{F}_{\mathrm{BB}})$ and $(\mathcal{W}_{\mathrm{RF}},\ \mathcal{W}_{\mathrm{BB}})$, the received signal in (4) can be reexpressed as

$$\begin{aligned} y=\sqrt{P}\mathcal{W}^H_{\mathrm{BB}(s_\mathrm{r},i_\mathrm{r})}\bar{\mathcal{W}}^H_{\mathrm{RF}(s_\mathrm{r},i_\mathrm{r})}\mathbf{H}\bar{\mathcal{F}}_{\mathrm{RF}(s_\mathrm{t},i_\mathrm{t})}\mathcal{F}_{\mathrm{BB}(s_\mathrm{t},i_\mathrm{t})}d \\ +\mathcal{W}^H_{\mathrm{BB}(s_\mathrm{r},i_\mathrm{r})}\bar{\mathcal{W}}^H_{\mathrm{RF}(s_\mathrm{r},i_\mathrm{r})}\mathbf{n}, \end{aligned} \tag{37}$$

where $\mathcal{F}_{\mathrm{BB}(s_\mathrm{t},i_\mathrm{t})}$ denotes the i_t-th codeword of the s-th layer in the digital codebook used at the transmitter, which is an R-element column vector. Following the definition of $\mathbf{F}_{\mathrm{RF}}$ in (2), $\bar{\mathcal{F}}_{\mathrm{RF}(s_\mathrm{t},i_\mathrm{t})}$ is a block diagonal matrix, which is constructed with the $(s_\mathrm{t}, i_\mathrm{t})$-th codeword $\mathcal{F}_{\mathrm{RF}(s_\mathrm{t},i_\mathrm{t})}$ of the analog codebook $\mathcal{F}_{\mathrm{RF}}$. $\mathcal{W}_{\mathrm{BB}(s_\mathrm{r},i_\mathrm{r})}$ and $\bar{\mathcal{W}}_{\mathrm{RF}(s_\mathrm{r},i_\mathrm{r})}$ have similar definitions as $\mathcal{F}_{\mathrm{BB}(s_\mathrm{t},i_\mathrm{t})}$ and $\bar{\mathcal{F}}_{\mathrm{RF}(s_\mathrm{t},i_\mathrm{t})}$, respectively.

The proposed three-phase beam alignment scheme is summarized in Algorithm 2, in which the initial layer s_I is determined in the 2-nd line. The beamwidth of the s_I-th layer is initialized according to the input parameters N, R, and s_I, followed by $i^{\mathrm{r}}_{\min}$, $i^{\mathrm{r}}_{\max}$ and $i^{\mathrm{t}}_{\min}$, $i^{\mathrm{t}}_{\max}$. The pseudo-code between the 4-th and the 9-th lines is associated with the initial setup phase, the content from the 11-th line to the 17-th line corresponds to the hierarchical transmission beam searching, and the rest is developed for the hierarchical beam searching at the receiver.

C. ANALYSIS ON TRAINING OVERHEAD

Generally, the number of time slots consumed on the initial setup phase is $|\mathcal{I}^{\mathrm{r}}_{\mathrm{AS}}(s_\mathrm{I})||\mathcal{I}^{\mathrm{t}}_{\mathrm{AS}}(s_\mathrm{I})|$. Both the second phase and the third phase consume the time slots of $2(S-s_\mathrm{I})$. Thus, the entire overhead of the proposed beam alignment scheme is $|\mathcal{I}^{\mathrm{r}}_{\mathrm{AS}}(s_\mathrm{I})||\mathcal{I}^{\mathrm{t}}_{\mathrm{AS}}(s_\mathrm{I})|+4(S-s_\mathrm{I})$. When $s_\mathrm{I}=1$ and no angle supports are available at the transceiver, the overhead will increase to $N^2/(4^{\lfloor\log_2 R\rfloor})+8\lfloor\log_2 R\rfloor$, which yields $(N/R)^2+8\log_2 R$ when R is an integer power of 2.

V. NUMERICAL RESULTS

In this section, we evaluate the performance of the proposed DFT codebook design and the beam alignment scheme with numerical results, which includes beam coverage, angle estimation success ratio and effective spectrum efficiency.

Algorithm 2 Proposed Beam Alignment Algorithm

Input: $P/\sigma_{\mathrm{n}}^2, P_{\mathrm{FA}}, \mathcal{D}_{\mathrm{AS}}^{\mathrm{r}}, \mathcal{D}_{\mathrm{AS}}^{\mathrm{t}}, N, R, \mathcal{W}_{\mathrm{BB}}, \mathcal{W}_{\mathrm{RF}}, \mathcal{F}_{\mathrm{BB}}, \mathcal{F}_{\mathrm{RF}}$
Output: $i_{\mathrm{r}}^{\star}, i_{\mathrm{t}}^{\star}$

Initialize: $P_{\mathrm{v}}=0$; $S=2\lfloor \log_2 R \rfloor + 1$; $|\alpha_{\mathrm{LS}}|=1$;
Determine s_{I} by using (36); $B_{s_{\mathrm{I}}}^{\mathrm{r}} = B_{s_{\mathrm{I}}}^{\mathrm{t}} = 4R/(N2^{s_{\mathrm{I}}})$;
Obtain $i_{\min}^{\mathrm{r}}$, $i_{\max}^{\mathrm{r}}$ and $i_{\min}^{\mathrm{t}}$, $i_{\max}^{\mathrm{t}}$ by using (31);
Exhaustive searching in the first layer:
for $i_t = i_{\min}^{t} : i_{\max}^{t}$ **do**
  for $i_r = i_{\min}^{r} : i_{\max}^{r}$ **do**
    $y = \sqrt{P}\mathcal{W}_{\mathrm{BB}(s_{\mathrm{I}},i_{\mathrm{r}})}^{H}\bar{\mathcal{W}}_{\mathrm{RF}(s_{\mathrm{I}},i_{\mathrm{r}})}^{H}\mathbf{H}\bar{\mathcal{F}}_{\mathrm{RF}(s_{\mathrm{I}},i_{\mathrm{t}})}\mathcal{F}_{\mathrm{BB}(s_{\mathrm{I}},i_{\mathrm{t}})}$
      $+ \mathcal{W}_{\mathrm{BB}(s_{\mathrm{I}},i_{\mathrm{r}})}^{H}\bar{\mathcal{W}}_{\mathrm{RF}(s_{\mathrm{I}},i_{\mathrm{r}})}^{H}\mathbf{n}$;
    if $|y|^2 > P_v$ **then**
      $P_{\mathrm{v}} = |y|^2, \hat{i}_{\mathrm{r}} = i_{\mathrm{r}}, \hat{i}_{\mathrm{t}} = i_{\mathrm{t}}$;
$i_{\mathrm{r}}' = \hat{i}_{\mathrm{r}}$, Feedback $i_{\mathrm{t}}' = \hat{i}_{\mathrm{t}}$;
for $s = s_I + 1 : S$ **do**
  for $i_t = 2i_t' - 1 : 2i_t'$ **do**
    $y = \sqrt{P}\mathcal{W}_{\mathrm{BB}(s_{\mathrm{I}},i_{\mathrm{r}}')}^{H}\bar{\mathcal{W}}_{\mathrm{RF}(s_{\mathrm{I}},i_{\mathrm{r}}')}^{H}\mathbf{H}\bar{\mathcal{F}}_{\mathrm{RF}(s,i_{\mathrm{t}})}\mathcal{F}_{\mathrm{BB}(s,i_{\mathrm{t}})}$
      $+ \mathcal{W}_{\mathrm{BB}(s_{\mathrm{I}},i_{\mathrm{r}}')}^{H}\bar{\mathcal{W}}_{\mathrm{RF}(s_{\mathrm{I}},i_{\mathrm{r}}')}^{H}\mathbf{n}$;
    if $|y|^2 > P_v$ **then**
      $P_{\mathrm{v}} = |y|^2, \hat{i}_{\mathrm{t}} = i_{\mathrm{t}}$;
  Feedback $i_{\mathrm{t}}' = \hat{i}_{\mathrm{t}}$;
$i_{\mathrm{t}}^{\star} = i_{\mathrm{t}}'$;
for $s = s_I + 1 : S$ **do**
  for $i_r = 2i_r' - 1 : 2i_r'$ **do**
    $y = \sqrt{P}\mathcal{W}_{\mathrm{BB}(s,i_{\mathrm{r}})}^{H}\bar{\mathcal{W}}_{\mathrm{RF}(s,i_{\mathrm{r}})}^{H}\mathbf{H}\bar{\mathcal{F}}_{\mathrm{RF}(S,i_{\mathrm{t}}^{\star})}\mathcal{F}_{\mathrm{BB}(S,i_{\mathrm{t}}^{\star})}$
      $+ \mathcal{W}_{\mathrm{BB}(s,i_{\mathrm{r}})}^{H}\bar{\mathcal{W}}_{\mathrm{RF}(s,i_{\mathrm{r}})}^{H}\mathbf{n}$;
    if $|y|^2 > P_v$ **then**
      $P_{\mathrm{v}} = |y|^2, \hat{i}_{\mathrm{r}} = i_{\mathrm{r}}$;
  $i_{\mathrm{r}}' = \hat{i}_{\mathrm{r}}$;
$i_{\mathrm{r}}^{\star} = i_{\mathrm{r}}'$;
Return $i_{\mathrm{r}}^{\star}, i_{\mathrm{t}}^{\star}$;

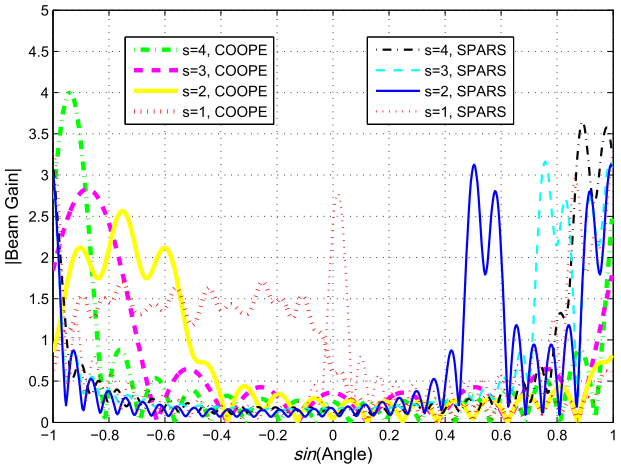

FIGURE 4. The beam coverage comparison between the proposed DFT codebook and the SPARS codebook, where $R = 4$, $N = 8$.

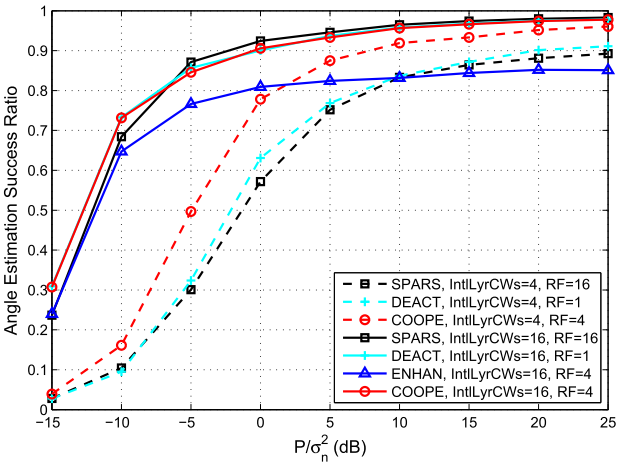

FIGURE 5. The angle-estimation-success-ratio comparison between different codebooks with different layers for the initial training phase, in which $RN = 64$.

Fig. 4 demonstrates the beam coverage of the first codewords at the different layers in the proposed subarray-cooperation-based DFT codebook (marked as COOPE), in which each of $R = 4$ subarrays consists of $N = 8$ antennas. It can be found that the beam coverage satisfies the hierarchical relationship of a binary-tree codebook. In contrast to the SPARS method for an ($RN = 32$)-element array [16], the beam patterns of the proposed codebook are more flat than those of the SPARS codebook, which is subject to beam sinks in relatively low layers when the number of RF chain R is limited. We compare the proposed codebook with the SPARS scheme under the condition of equal RF chains ($R = 4$) and the same array scale ($RN = 32$), although the SPARS codebook was proposed for fully-connected structures, where all the RN phase shifters were available for each RF chain.

The performance of the proposed codebook is further evaluated by using Algorithm 2 in Fig. 5 and Fig. 6, in which both transmitter and receiver are equipped with $R = 4$ ULA subarrays, and each subarray has $N = 16$ antennas with half-wavelength antenna spacing. We adopt the geometric channel model with $L = 3$ paths. Specifically, the power of the LoS component is 20 dB higher than that of a NLoS path, which obeys complex Gaussian distribution. The physical AoDs/AoAs of the MPCs are randomly distributed on $[-\pi/2, \pi/2)$. All the numerical results are obtained by averaging over 10^4 channel realizations.

Fig. 5 compares the proposed DFT codebook with different counterparts in terms of the angle estimation success ratios under different transmission SNRs. The schemes of SPARS, DEACT, and ENHAN denote the sparse, deactivation and beam enhancement methods, which were proposed in [16], [22], and [29], respectively. As shown in Fig. 5, the success ratios grow with the increasing SNRs for all schemes. Furthermore, the success ratios of the proposed scheme are higher than those of other counterparts over the whole SNR ranges when the number of the codewords in

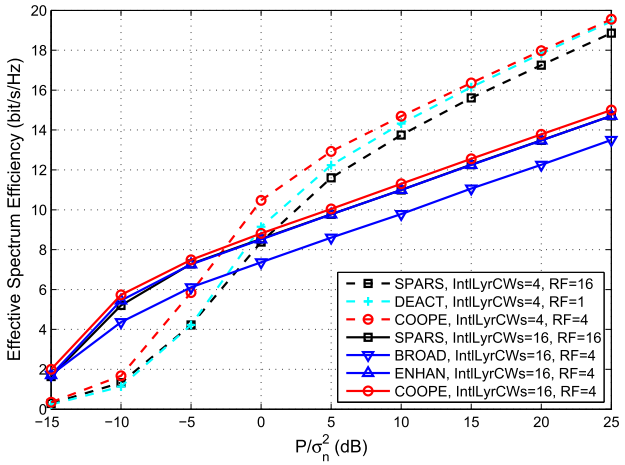

FIGURE 6. The effective-spectrum-efficiency comparison between different codebooks with different layers for the initial training phase, where the codebook "BROAD" proposed in [29], $RN = 64$.

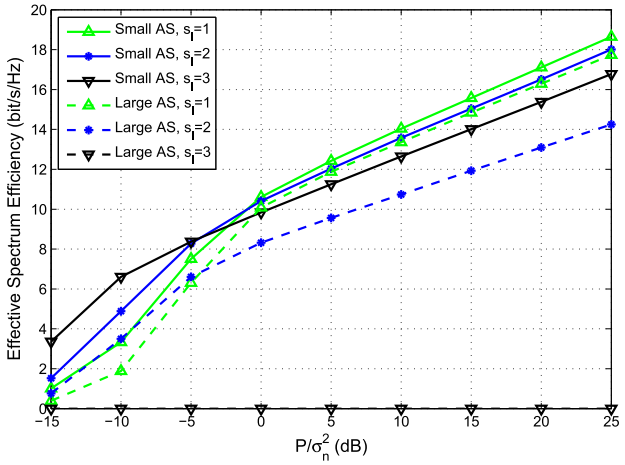

FIGURE 7. The effective spectrum efficiency of the proposed beam alignment scheme with different initial searching layers under different angle supports, where $R = 4$, $N = 16$, $T = 256$, "Small AS" and "Large AS" representing the physical angle supports of $\mathcal{D}'^{\mathrm{r}}_{\mathrm{AS}} = \mathcal{D}'^{\mathrm{t}}_{\mathrm{AS}} = [-\pi/12,\ \pi/12)$ and $\mathcal{D}'^{\mathrm{r}}_{\mathrm{AS}} = \mathcal{D}'^{\mathrm{t}}_{\mathrm{AS}} = [-5\pi/12,\ 5\pi/12)$, respectively.

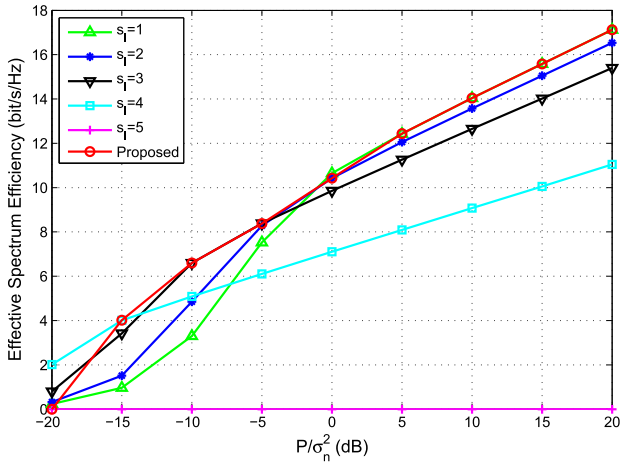

FIGURE 8. Performance comparison between the proposed scheme and the methods using fixed layers for the initial searching, where $T = 256$.

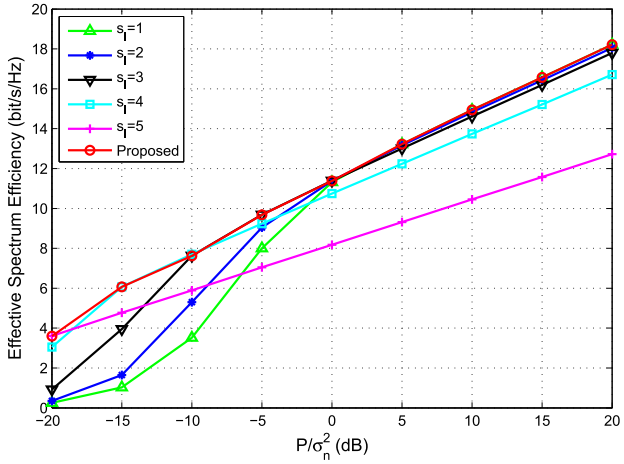

FIGURE 9. Performance comparison between the proposed scheme and the methods using fixed layers for the initial searching, where $T = 1,024$.

the initial layer (marked as IntlLyrCWs) is 4 (corresponding to the initial layer s_{I}=1). For all the involved codebooks, straightforwardly, the beam alignments starting with the relatively high layer (s_{I}=3, IntlLyrCWs=16) perform better than those starting with the low layer (s_{I}=1, IntlLyrCWs=4) due to high SNRs. Additionally, it can be observed that the saturation of success rate will occur once the transmission power is sufficiently large owing to the spatial fading.

The effective-spectrum-efficiency comparison between different schemes is provided in Fig. 6, in which the number of total time slots is set as 1,024. For the same number of the training codewords adopted in the initial phase, the spectrum efficiency of the proposed scheme is higher than those of all benchmarks. The superiority of the proposed scheme is more significant when the number of the codewords in the initial searching phase is small, benefitting from both large array gain and flat beam pattern in low layers. Moreover, this advantage is notable in the regime of low-medium SNRs, since the large beam gain is vital for the correct beam alignment. Note that the spectrum efficiency of the SPARS method is lower than that of the proposed scheme due to its sacrificed beam gain, even though the higher angle detection success ratio may be achieved by the SPARSE method.

Fig. 7 depicts the effective spectrum efficiency of the proposed beam alignment scheme with different layers for the initial training phase under different angle supports, where the size of entire transmission block is 256. With the limited transmission block, it is intuitive that the spectrum efficiency corresponding to the small angle supports is higher than that associated with the large angle supports when the same initial layers s_{I} are adopted. It can be found that the best spectrum efficiency at different SNRs may be achieved by different s_{I} for a given angle support, which implies that the initial layers should be adaptively selected under different SNRs to maintain sufficient transceiver gain.

$$
\begin{aligned}
&G(\mathbf{f}_s', \tilde{\Phi}_{s,r}) \mid_{\mathbf{f}_{s,r}^{\mathrm{RF}}=\mathbf{a}(N,\Phi_{s,r}),\ 1\le r\le \hat{R}_s} \\
&\overset{(a)}{\approx} G(\mathbf{f}_s', \tilde{\Phi}_{s,r}) \mid_{\mathbf{f}_{s,r'}^{\mathrm{RF}}=\mathbf{a}(N,\Phi_{s,r'}),\ r'=r-1,\ r,\ 1<r\le \hat{R}_s.} \\
&\overset{(b)}{=} \sum_{r'=r-1}^{r} \frac{1}{\sqrt{\hat{R}_s N}} \frac{\sin\left[\pi N(\tilde{\Phi}_{s,r}-\Phi_{s,r'})/2\right]}{\sin\left[\pi(\tilde{\Phi}_{s,r}-\Phi_{s,r'})/2\right]} e^{\{-j\pi[(r-1)N\tilde{\Phi}_{s,r}+(N-1)(\tilde{\Phi}_{s,r}-\Phi_{s,r'})/2]+j\theta_r'\}} \\
&\overset{(c)}{=} \frac{1}{\sqrt{\hat{R}_s N}} \frac{\sin[\pi/2]}{\sin[\pi/(2N)]} e^{\{-j\pi[(r-2)N\tilde{\Phi}_{s,r}+(N-1)/(2N)]+j\theta_{r-1}\}} + \frac{1}{\sqrt{\hat{R}_s N}} \frac{\sin[-\pi/2]}{\sin[-\pi/(2N)]} e^{\{-j\pi[(r-1)N\tilde{\Phi}_{s,r}-(N-1)/(2N)]+j\theta_r\}}
\end{aligned} \tag{38}
$$

$$
\begin{aligned}
&\angle G(\mathbf{f}_{s,r}^{\mathrm{RF}}, \tilde{\Phi}_{s,r}) - \angle G(\mathbf{f}_{s,r-1}^{\mathrm{RF}}, \tilde{\Phi}_{s,r}) \\
&\overset{(a)}{=} \theta_r - \theta_{r-1} + (N-1)\pi/(2N) + (N-1)\pi/(2N) - \pi[(r-1)N\tilde{\Phi}_{s,r}] + \pi[(r-2)N\tilde{\Phi}_{s,r}] \\
&= \theta_r - \theta_{r-1} + (N-1)\pi/N - \pi N\tilde{\Phi}_{s,r} \\
&\overset{(b)}{=} \theta_r - \theta_{r-1} + (N-1)\pi/N + N\pi - 2(r-1)\pi
\end{aligned} \tag{39}
$$

The effective-spectrum-efficiency comparison between the proposed scheme and the methods using the fixed initial layers under small $T = 256$ and large $T = 1,024$ are illustrated in Fig. 8 and Fig. 9, respectively, in which $R = 4$, $N = 16$, the angle supports in physical angle domain are $\mathcal{D}_{\mathrm{AS}}^{'\mathrm{r}} = \mathcal{D}_{\mathrm{AS}}^{'\mathrm{t}} = [-\pi/12,\ \pi/12)$, $P_{\mathrm{FA}} = 0.01$.

As shown in Fig. 8, the proposed scheme selects the layers $s_{\mathrm{I}} = \{4,\ 3,\ 2,\ 2\}$ and 1 corresponding to the transmission SNRs $P/\sigma_{\mathrm{n}}^2 = \{-15,\ -10,\ -5,\ 0\}$ and $P/\sigma_{\mathrm{n}}^2 \ge 5$ for initial training, respectively. It can be found that the proposed scheme can adaptively select the initial layers under different P/σ_{n}^2, such that it outperforms the other methods using the fixed initial layer over the whole transmission SNRs. For low transmission SNRs, the proposed scheme chooses relatively high layers to obtain large transceiver gain, which is essential to guarantee sufficient angle detection success ratio. With growing P/σ_{n}^2, the relatively low layers are selected to reduce the searching overhead, since the overhead becomes a considerable factor on spectrum efficiency when T is limited.

Similar conclusions can be drawn from Fig. 9 as that obtained in Fig. 8. Specifically, the proposed scheme appears to select the highest layer when the transmission SNRs are extremely low, i.e., exhaustive beam searching is conducted. It is natural that the dominant contribution on effective spectrum efficiency is large transceiver gain rather than the training overhead when T is large enough.

VI. CONCLUSION

This paper has investigated a subarray-cooperation-based multi-resolution codebook design and adaptive beam alignment for mmWave backhaul links in the context of FDD systems, in which the AWV of each subarray is configured as an N-element DFT vector, and the inter-subarray cooperation is achieved by the digital beamformer. Consequently, the hardware complexity is significantly reduced. With the multi-subarray cooperation, the proposed multi-resolution codebook provides flat beam pattern and harvests the array gain at the lowest layer. Moreover, the predictable transceiver gain is exploited to adaptively select the initial layers under different transmission SNRs, which guarantees sufficient success ratios on angle detection. Simulation results verify the effectiveness of the proposed beam alignment scheme.

APPENDIX
PROOF OF PROPOSITION 3

Proof: Since the complete beam gain at $\tilde{\Phi}_{s,r}$ mainly depends on that of two adjacent sub-beams, namely, the $(r-1)$-th sub-beam and the r-th sub-beam, the complete beam gain can be approximately expressed as (38), shown at the top of this page, where (a) holds for the assumption of the approximation, (b) uses the result of (22), (c) jointly leverages the configurations in Proposition 1 and (23), respectively. Therefore, the phase difference between two beam-gains of the adjacent sub-beams can be written as (39), shown at the top of this page, where (a) comes from the amplitudes of these terms being positive, (b) holds for the setting in (23), respectively. Thus, we can obtain $\theta_r - \theta_{r-1} = -(N-1)\pi/N$ to guarantee constructive cooperation between adjacent sub-arrays at their intersection. Consequently, we have (24). ■

REFERENCES

[1] Z. Pi and F. Khan, "An introduction to millimeter-wave mobile broadband systems," *IEEE Commun. Mag.*, vol. 49, no. 6, pp. 101–107, Jun. 2011.

[2] S. Rangan, T. S. Rappaport, and E. Erkip, "Millimeter-wave cellular wireless networks: Potentials and challenges," *Proc. IEEE*, vol. 102, no. 3, pp. 366–385, Mar. 2014.

[3] Y. Han, H. Zhang, S. Jin, X. Li, R. Yu, and Y. Zhang, "Investigation of transmission schemes for millimeter-wave massive MU-MIMO systems," *IEEE Syst. J.*, vol. 11, no. 1, pp. 72–83, Mar. 2017.

[4] T. S. Rappaport, Y. Qiao, J. I. Tamir, J. N. Murdock, and E. Ben-Dor, "Cellular broadband millimeter wave propagation and angle of arrival for adaptive beam steering systems (invited paper)," in *Proc. IEEE Radio Wireless Symp. (RWS)*, Jan. 2012, pp. 151–154.

[5] T. S. Rappaport, F. Gutierrez, Jr., E. Ben-Dor, J. N. Murdock, Y. Qiao, and J. I. Tamir, "Broadband millimeter-wave propagation measurements and models using adaptive-beam antennas for outdoor urban cellular communications," *IEEE Trans. Antennas Propag.*, vol. 61, no. 4, pp. 1850–1859, Apr. 2013.

[6] T. S. Rappaport *et al.*, "Millimeter wave mobile communications for 5G cellular: It will work!" *IEEE Access*, vol. 1, pp. 335–349, 2013.

[7] C. Lin and G. Y. L. Li, "Terahertz communications: An array-of-subarrays solution," *IEEE Commun. Mag.*, vol. 54, no. 12, pp. 124–131, Dec. 2016.

[8] S. A. Busari, K. M. S. Huq, S. Mumtaz, L. Dai, and J. Rodriguez, "Millimeter-wave massive MIMO communication for future wireless systems: A survey," *IEEE Commun. Surveys Tuts.*, vol. 20, no. 2, pp. 836–869, 2nd Quart., 2018.

[9] W. Roh *et al.*, "Millimeter-wave beamforming as an enabling technology for 5G cellular communications: Theoretical feasibility and prototype results," *IEEE Commun. Mag.*, vol. 52, no. 2, pp. 106–113, Feb. 2014.

[10] R. W. Heath, Jr., and N. González-Prelcic, S. Rangan, W. Roh, and A. M. Sayeed, "An overview of signal processing techniques for millimeter wave MIMO systems," *IEEE J. Sel. Topics Signal Process.*, vol. 10, no. 3, pp. 436–453, Apr. 2016.

[11] C. Lin and G. Y. Li, "Energy-efficient design of indoor mmWave and sub-THz systems with antenna arrays," *IEEE Trans. Wireless Commun.*, vol. 15, no. 7, pp. 4660–4672, Jul. 2016.

[12] A. Alkhateeb, G. Leus, and R. W. Heath, Jr., "Limited feedback hybrid precoding for multi-user millimeter wave systems," *IEEE Trans. Wireless Commun.*, vol. 14, no. 11, pp. 6481–6494, Nov. 2015.

[13] H. He, C.-K. Wen, S. Jin, and G. Y. Li, "Deep learning-based channel estimation for beamspace mmWave massive MIMO systems," *IEEE Wireless Commun. Lett.*, vol. 7, no. 5, pp. 852–855, Oct. 2018.

[14] O. El Ayach, S. Rajagopal, S. Abu-Surra, Z. Pi, and R. W. Heath, Jr., "Spatially sparse precoding in millimeter wave MIMO systems," *IEEE Trans. Wireless Commun.*, vol. 13, no. 3, pp. 1499–1513, Mar. 2014.

[15] Y. Huang, J. Zhang, and M. Xiao, "Constant envelope hybrid precoding for directional millimeter-wave communications," *IEEE J. Sel. Areas Commun.*, vol. 36, no. 4, pp. 845–859, Apr. 2018.

[16] A. Alkhateeb, O. El Ayach, G. Leus, and R. W. Heath, Jr., "Channel estimation and hybrid precoding for millimeter wave cellular systems," *IEEE J. Sel. Topics Signal Process.*, vol. 8, no. 5, pp. 831–846, Oct. 2014.

[17] Z. Xiao, H. Dong, L. Bai, P. Xia, and X.-G. Xia, "Enhanced channel estimation and codebook design for millimeter-wave communication," *IEEE Trans. Veh. Technol.*, vol. 67, no. 10, pp. 9393–9405, Oct. 2018.

[18] S. He, J. Wang, Y. Huang, B. Ottersten, and W. Hong, "Codebook-based hybrid precoding for millimeter wave multiuser systems," *IEEE Trans. Signal Process.*, vol. 65, no. 20, pp. 5289–5304, Oct. 2017.

[19] K. Chen and C. Qi, "Beam training based on dynamic hierarchical codebook for millimeter wave massive MIMO," *IEEE Commun. Lett.*, vol. 23, no. 1, pp. 132–135, Jan. 2019.

[20] R. Zhang, H. Zhang, and W. Xu, "Analog codebook design for mmWave communications with an auxiliary phase shifter group," in *Proc. 10th Int. Conf. Wireless Commun. Signal Process. (WCSP)*, Hangzhou, China, Oct. 2018, pp. 1–6.

[21] S. Noh, M. D. Zoltowski, Y. Sung, and D. J. Love, "Pilot beam pattern design for channel estimation in massive MIMO systems," *IEEE J. Sel. Topics Signal Process.*, vol. 8, no. 5, pp. 787–801, Oct. 2014.

[22] J. Wang *et al.*, "Beam codebook based beamforming protocol for multi-Gbps millimeter-wave WPAN systems," *IEEE J. Sel. Areas Commun.*, vol. 27, no. 8, pp. 1390–1399, Oct. 2009.

[23] S. Hur, T. Kim, D. J. Love, J. V. Krogmeier, T. A. Thomas, and A. Ghosh, "Millimeter wave beamforming for wireless backhaul and access in small cell networks," *IEEE Trans. Commun.*, vol. 61, no. 10, pp. 4391–4403, Oct. 2013.

[24] Z. Xiao, T. He, P. Xia, and X.-G. Xia, "Hierarchical codebook design for beamforming training in millimeter-wave communication," *IEEE Trans. Wireless Commun.*, vol. 15, no. 5, pp. 3380–3392, May 2016.

[25] Z. Xiao, P. Xia, and X.-G. Xia, "Codebook design for millimeter-wave channel estimation with hybrid precoding structure," *IEEE Trans. Wireless Commun.*, vol. 16, no. 1, pp. 141–153, Jan. 2017.

[26] J. Zhang, Y. Huang, Q. Shi, J. Wang, and L. Yang, "Codebook design for beam alignment in millimeter wave communication systems," *IEEE Trans. Commun.*, vol. 65, no. 11, pp. 4980–4995, Nov. 2017.

[27] S. Noh, M. D. Zoltowski, and D. J. Love, "Multi-resolution codebook and adaptive beamforming sequence design for millimeter wave beam alignment," *IEEE Trans. Wireless Commun.*, vol. 16, no. 9, pp. 5689–5701, Sep. 2017.

[28] Y. Han, S. Jin, J. Zhang, J. Zhang, and K.-K. Wong, "DFT-based hybrid beamforming multiuser systems: Rate analysis and beam selection," *IEEE J. Sel. Topics Signal Process.*, vol. 12, no. 3, pp. 514–528, Jun. 2018.

[29] C. Lin and G. Y. Li, "Coordinated beamforming training for mmWave and sub-THz communications with antenna subarrays," in *Proc. IEEE Wireless Commun. Netw. Conf. (WCNC)*, San Francisco, CA, USA, Mar. 2017, pp. 1–6.

[30] C. Lin, G. Y. Li, and L. Wang, "Subarray-based coordinated beamforming training for mmWave and sub-THz communications," *IEEE J. Sel. Areas Commun.*, vol. 35, no. 9, pp. 2115–2126, Sep. 2017.

RENMIN ZHANG (S'17) received the B.S. degree in electrical engineering from the Guilin University of Electronic Technology, Guilin, China, in 2003, and the M.S. degree in electronic and communication engineering from Peking University, Beijing, China, in 2011. He is currently pursuing the Ph.D. degree in communication and information systems with the School of Information Science and Engineering, Southeast University, Nanjing, China.

From 2003 to 2013, he was with Huaihua University, Huaihua, China, first as an Assistant and then as a Lecturer, where he has been an Associate Professor with the Hunan Provincial Key Laboratory of Ecological Agriculture Intelligent Control Technology, since 2013. His current research interests include mmWave and THz communications, multiuser MIMO, statistical signal processing, and machine learning for wireless communications.

HUA ZHANG (M'04) received the B.S. and M.S. degrees from the Department of Radio Engineering, Southeast University, Nanjing, China, in 1998 and 2001, respectively, and the Ph.D. degree from the School of Electrical and Computer Engineering, Georgia Institute of Technology, Atlanta, GA, USA, in 2004, where he was a Graduate Research Assistant, from 2001 to 2004.

From 2004 to 2005, he was a Senior System Engineer with Skyworks Solutions, Inc., Irvine, CA, USA. From 2005 to 2006, he was a Staff Engineer with MaxLinear, Inc., Carlsbad, CA, USA. He is currently a Professor with the National Mobile Communications Research Laboratory, Southeast University, Nanjing, China. His current research interests include massive MIMO, software-defined radio, and cooperative communications. He received the Best Paper Awards from the IEEE MAPE, in 2013, and the IEEE GLOBECOM, in 2014.

WEI XU (S'07–M'09–SM'15) received the B.Sc. degree in electrical engineering and the M.S. and Ph.D. degrees in communication and information engineering from Southeast University, Nanjing, China, in 2003, 2006, and 2009, respectively. From 2009 to 2010, he was a Postdoctoral Research Fellow with the Department of Electrical and Computer Engineering, University of Victoria, Canada. He is currently a Professor with the National Mobile Communications Research Laboratory, Southeast University.

He has co-authored over 80 refereed journal papers in addition to 28 granted domestic patents and three U.S. patents. His research interests include cooperative communications, information theory, signal processing, and machine learning for wireless communications. He received the Best Paper Awards from IEEE MAPE, in 2013, IEEE/CIC ICCC, in 2014, IEEE GLOBECOM, in 2014, IEEE ICUWB, in 2016, and WCSP, in 2017. He was a co-recipient of the First Prize of the Science and Technology Award in Jiangsu Province, China, in 2014. He has been involved in technical program committees for international conferences, including IEEE GLOBECOM, IEEE ICC, IEEE WCNC, IEEE VTC, and IEEE PIMRC. He was an Editor of the IEEE COMMUNICATIONS LETTERS, from 2012 to 2017, and he is currently an Editor of the IEEE TRANSACTIONS ON COMMUNICATIONS and the IEEE ACCESS.

XIAOHU YOU (F'12) received the B.S., M.S., and Ph.D. degrees in electrical engineering from the Nanjing Institute of Technology, Nanjing, China, in 1982, 1985, and 1989, respectively.

From 1987 to 1989, he was with the Nanjing Institute of Technology as a Lecturer. Since 1990, he has been with Southeast University, Nanjing, first as an Associate Professor and later as a Professor. He is currently the Chief of the Technical Group of the China 3G/B3G Mobile Communication R&D Project. His research interests include mobile communications, adaptive signal processing, and artificial neural networks, with applications to communications and biomedical engineering. He received the Excellent Paper Prize from the China Institute of Communications, in 1987, and the Elite Outstanding Young Teachers Awards from Southeast University, in 1990, 1991, and 1993. He also received the 1989 Young Teacher Award from the Fok Ying Tung Education Foundation, State Education Commission of China.